

The anti-apoptotic protein HAX-1 is a regulator of cardiac function

Wen Zhao^{a,1}, Jason R. Waggoner^{a,1}, Zhi-Guo Zhang^{a,b,1}, Chi Keung Lam^a, Peidong Han^a, Jiang Qian^a, Paul M. Schroder^a, Bryan Mitton^a, Aikaterini Kontrogianni-Konstantopoulos^c, Seth L. Robia^d, and Evangelia G. Kranias^{a,e,2}

^aDepartment of Pharmacology and Cell Biophysics, University of Cincinnati College of Medicine, Cincinnati, OH 45267-0575; ^bDepartment of Physiology and Pathophysiology, Peking University Health Science Center, Beijing, China, 100083; ^cDepartment of Biochemistry and Molecular Biology, University of Maryland School of Medicine, Baltimore, MD 21201; ^dDepartment of Physiology, Loyola University Chicago, Maywood, IL 60153; and ^eMolecular Biology Divisions, Center for Basic Research, Foundation for Biomedical Research of the Academy of Athens, Athens 115 27, Greece

Edited by David H. MacLennan, University of Toronto, Toronto, Canada, and approved October 14, 2009 (received for review June 23, 2009)

The HS-1 associated protein X-1 (HAX-1) is a ubiquitously expressed protein that protects cardiomyocytes from programmed cell death. Here we identify HAX-1 as a regulator of contractility and calcium cycling in the heart. HAX-1 overexpression reduced sarcoplasmic reticulum Ca-ATPase (SERCA2) pump activity in isolated cardiomyocytes and in vivo, leading to depressed myocyte calcium kinetics and mechanics. Conversely, downregulation of HAX-1 enhanced calcium cycling and contractility. The inhibitory effects of HAX-1 were abolished upon phosphorylation of phospholamban, which plays a fundamental role in controlling basal contractility and constitutes a key downstream effector of the β -adrenergic signaling cascade. Mechanistically, HAX-1 promoted formation of phospholamban monomers, the active/inhibitory units of the calcium pump. Indeed, ablation of PLN rescued HAX-1 inhibition of contractility in vivo. Thus, HAX-1 represents a regulatory mechanism in cardiac calcium cycling and its responses to sympathetic stimulation, implicating its importance in calcium homeostasis and cell survival.

calcium | cardiomyocytes | contractility | phospholamban | sarcoplasmic reticulum

Heart failure, the leading cause of human morbidity and mortality with estimated 550,000 new cases annually, is characterized by myocardial remodeling and left ventricular dysfunction. A universal characteristic of human and experimental heart failure is depressed sarcoplasmic reticulum (SR) calcium cycling, which is mainly related to decreased cardiac SR Ca-ATPase (SERCA2a) expression and increased inhibition of the Ca pump by phospholamban (PLN) (1–3). PLN is a small phosphoprotein, which represents a nodal point in calcium cycling and the heart's responses to β -agonists (4). However, it is not currently clear whether PLN mediates its regulatory effects on the calcium pump alone or if there are other proteins modulating its activity. Along these lines, we recently showed that PLN interacts with the anti-apoptotic protein HS-1 associated protein X-1 (HAX-1) in vitro (5), but the functional significance of this PLN binding partner in SR calcium cycling remains unclear.

HAX-1, an approximately 35-kDa protein, was originally identified as an intracellular anti-apoptotic protein (6). HAX-1 is not significantly homologous to any other proteins (6). It shares some similarity to Bcl-2 and related proteins, as well as to Nip3, a Bcl-2-interacting protein. HAX-1 also contains a putative PEST sequence (amino acids 104–117), which suggests rapid and regulated degradation of the protein. There are also some additional interesting features: an acid box (amino acids 30–41) with unknown function, composed mostly of glutamic and aspartic acids, as well as several recently identified protein-binding regions, that are present mostly in the C-terminal part of the protein (7). HAX-1 could protect cardiomyocytes from hypoxia-reoxygenation-induced apoptosis by inhibiting caspase-9 activation (8). The region of HAX-1 interacting with caspase-9 contains amino acids 174–206 (8), while its minimal binding region with PLN is amino acids 203–245, which is adjacent but separated from the caspase-9 binding domain (5).

Transient transfection of HAX-1 in HEK293 cells demonstrated that it preferentially localizes to mitochondria. However, upon cotransfection with PLN, it is present in the ER and colocalizes with PLN (5). Previous immunofluorescence microscopy studies have localized HAX-1 to the mitochondria and endoplasmic reticulum in COS-7, HeLa, and DG75 cells (6, 8–12), although two of these studies also localized HAX-1 to the nuclear envelope (6, 9). Overall, most of these studies focused on the anti-apoptotic function of HAX-1.

Given the importance of phospholamban in the heart's responses to β -adrenergic stimulation and the promise of PLN-targeted therapy to correct dysfunction of failing hearts, the identification of the interaction between HAX-1 and PLN represents a significant finding. Thus, it becomes critical to further characterize the functional significance of HAX-1 in vitro and in vivo, with specific emphasis of its regulatory roles on: a) PLN activity; and b) SR calcium cycling and contractility. To better understand these notions, the HAX-1 protein levels were altered in an acute or chronic manner in cardiomyocytes. Adenoviruses with sense or antisense HAX-1 gene were generated to infect adult cardiac cells. A transgenic mouse with cardiac specific overexpression of HAX-1 and a HAX-1 deficient model were also characterized to evaluate the functional significance of HAX-1 in vivo. Our results demonstrate that overexpression of HAX-1 decreases SR calcium transport, calcium content, and cardiac function through increased inhibition by PLN. Accordingly, downregulation of this protein augments cardiac contractile performance. These regulatory effects of HAX-1 are abolished in the absence of PLN in vivo. Thus, HAX-1 represents an additional regulator of SR calcium transport and contractility in the heart.

Results

Effects of Acute HAX-1 Overexpression and Downregulation in Adult Rat Cardiomyocytes. A previous study showed a direct interaction between PLN and HAX-1 in vitro, suggesting a role for HAX-1 in cardiac function. To examine the significance of HAX-1 in cardiac SR calcium cycling and contractility, adult rat ventricular cardiomyocytes were infected with adenoviruses expressing sense (HAX-1) or antisense HAX-1 (HAX-1-AS) (Fig. 1A). In initial experiments, we investigated the localization of HAX-1 in control and infected cardiomyocytes using immunofluorescence. Previous studies reported that HAX-1 localizes to both mitochondria and

Author contributions: W.Z. and E.G.K. designed research; W.Z., J.R.W., Z.-G.Z., C.K.L., P.H., J.Q., P.M.S., B.M., and S.L.R. performed research; W.Z., J.R.W., Z.-G.Z., C.K.L., P.H., J.Q., P.M.S., and S.L.R. analyzed data; and W.Z., J.R.W., A.K.-K., S.L.R., and E.G.K. wrote the paper.

The authors declare no conflict of interest.

This article is a PNAS Direct Submission.

¹W.Z., J.R.W., and Z.-G.Z. contributed equally to this work.

²To whom correspondence should be addressed. E-mail: litsa.kranias@uc.edu.

This article contains supporting information online at www.pnas.org/cgi/content/full/0906998106/DCSupplemental.

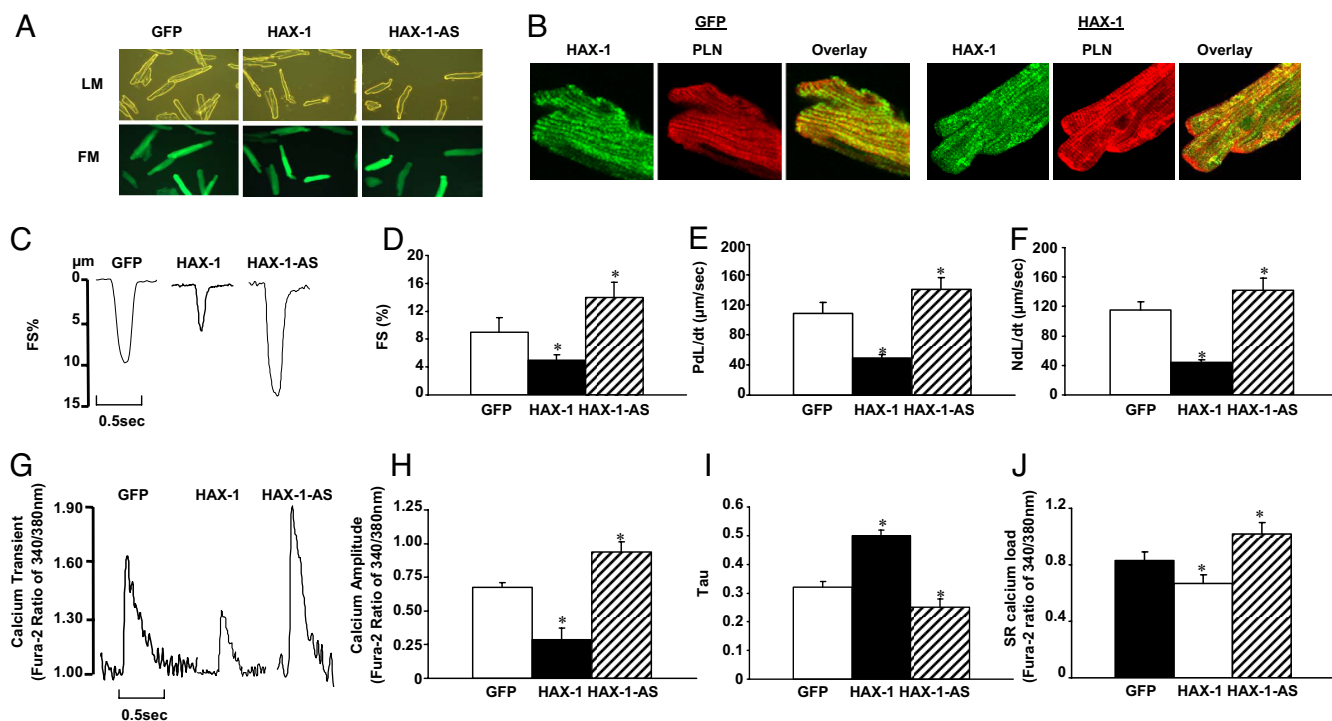


Fig. 1. Effects of acute HAX-1 overexpression or downregulation on rat cardiomyocyte contractile function. Adenoviruses with sense and anti-sense mouse HAX-1 gene insertion were generated according to standard procedures. An adenovirus expressing GFP was used as a control. Rat adult cardiomyocytes were isolated and infected with Ad.GFP (GFP), Ad.HAX-1 (HAX-1), and Ad.HAX-1-antisense (HAX-1-AS). (A) Representative images of infected cardiomyocytes under light microscopy (LM, upper panel) and fluorescence microscopy (FM, lower panel). (B) Immunofluorescence analysis of HAX-1 localization in GFP and HAX-1 infected cardiomyocytes, using PLN as a SR marker. To investigate the contractile function, myocytes were infected with GFP, HAX-1, and HAX-1-AS for 24 h and contractility was subsequently recorded. (C) Representative curves of myocyte contraction under basal conditions. (D) Percentage of fractional shortening (FS%), (E) rate of contraction (PdL/dt, $\mu\text{m}/\text{s}$), and (F) rate of relaxation (NdL/dt, $\mu\text{m}/\text{s}$) under basal conditions. For the calcium transients, cells were loaded with fura-2 for 30 min, and then calcium transients were recorded and analyzed. (G) Representative curves of calcium transients under basal conditions. (H) Calcium amplitude, indicated as the fura-2 ratio of 340/380 nm; (I) Tau under basal conditions. For SR calcium load indicating by caffeine-induced calcium release from SR, 10 mM caffeine was added to the buffer. (J) Peak of SR calcium load, indicated by the fura-2 ratio of 340/380 nm. $n = 4-5$ hearts (6-8 cells/heart) for each group. Data are mean \pm SEM. *, $P < 0.05$, compared to Ad.GFP group.

endoplasmic reticulum in different cell types, including COS-7, HeLa, and DG75 cells (6, 8-12). In cardiomyocytes, HAX-1 appeared to partially colocalize with PLN in control cells as well as in HAX-1 overexpressing cells (Fig. 1B).

Overexpression of HAX-1 (≈ 18 -fold, Fig. S1A) in rat adult cardiomyocytes resulted in significant decreases in fractional shortening, and the rates of contraction and relaxation to 43, 38, and 31%, respectively, compared to Ad.GFP infected cells (Fig. 1C-F). However, upon β -adrenergic-receptor stimulation by isoproterenol, phosphorylation of major phosphoproteins including phospholamban abolished the differences in the contractile parameters between control and HAX-1 overexpressing cells (Fig. S1C-E).

Consistent with the myocyte contractility data, the peak calcium was significantly depressed by HAX-1 overexpression and tau, a measure of Ca-decay rate, was prolonged to 163% of controls (Fig. 1G-I). These depressive effects of HAX-1 were abolished upon isoproterenol stimulation (Fig. S1F and G).

Assessment of SR calcium load by caffeine application revealed a 20% decrease, compared to control myocytes (Fig. 1J). However, there were no marked alterations of the SR calcium content upon isoproterenol stimulation, consistent with the calcium kinetic and mechanical parameters (Fig. S1H). These data indicate that acute overexpression of HAX-1 depresses cardiomyocyte calcium cycling and contractile performance under basal conditions, but isoproterenol prevents the inhibitory effects of HAX-1.

On the other hand, downregulation of HAX-1 (to 70% of control cells, Fig. S1B) was associated with significant increases in cardiomyocyte contractile parameters, including fractional shortening, rates of contraction and relaxation, to 156, 130, and 123%, respec-

tively, compared to controls (Fig. 1C-F). The calcium transients also showed significant enhancement (Fig. 1C-F). The peak calcium increased to 125% and tau was abbreviated to 72% of control cells, respectively (Fig. 1G-I). However, the contractile and calcium transient parameters were similar upon isoproterenol stimulation (Fig. S1C-G). Furthermore, caffeine-induced calcium release from SR was significantly enhanced to 130% of control cells under basal conditions (Fig. 1J), without significant alterations upon isoproterenol stimulation (Fig. S1H). These data indicate that acute downregulation of HAX-1 may enhance cardiomyocyte contractility and calcium transients under basal conditions.

Transgenic Overexpression of HAX-1 in the Mouse Heart. The results presented above indicated that acute alterations of HAX-1 expression have significant effects in cardiac calcium cycling and contractile performance. To further examine the functional role of HAX-1 in vivo, we generated a transgenic mouse model with cardiac specific HAX-1 overexpression (*OE*) (Fig. S2A). Quantitative Western blot analysis (Fig. 2A) of heart homogenates revealed that transgenesis resulted in approximately 2.5- and 2.3-fold increases of the HAX-1 protein levels in two different lines (L11 and L13). There were no significant alterations in cardiac morphology and histology by overexpression of HAX-1 at 3 months of age (Fig. S2B and C). Immunofluorescence analysis of the isolated mouse cardiomyocytes, using PLN as SR marker, indicated that the overexpressed HAX-1 colocalized with PLN (Fig. 2B), consistent with the adenoviral studies.

To examine the functional effects of HAX-1 overexpression in vivo, cardiomyocytes from line 11 were isolated and contractility as

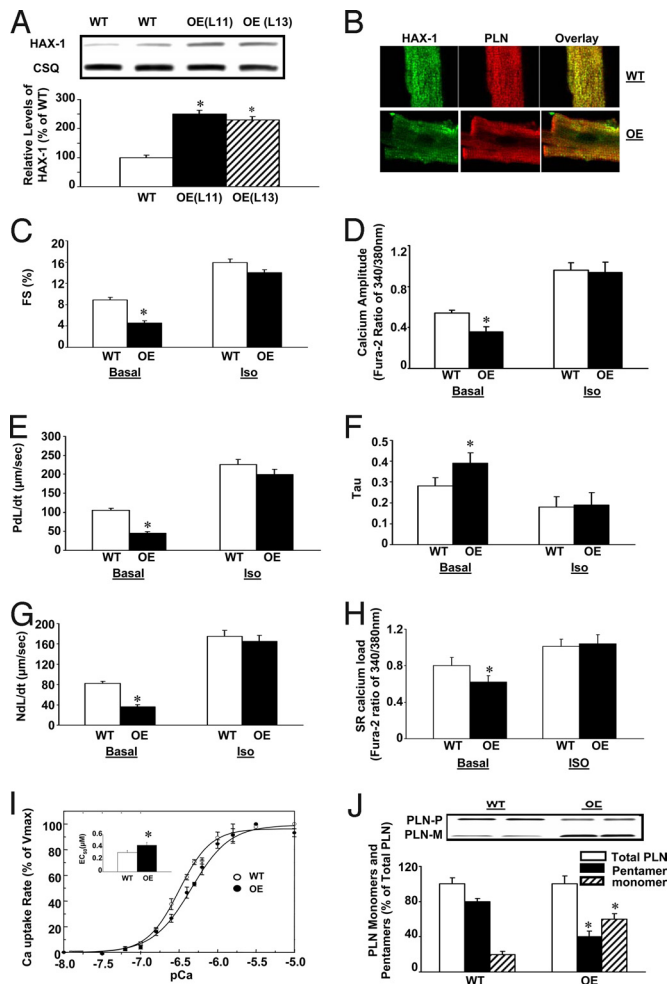


Fig. 2. Generation and characterization of cardiac-specific HAX-1 overexpressing mice. HAX-1 transgenic mice were generated, using mouse HAX-1 cDNA under the control of an α -MHC promoter and human growth hormone polyA (HGH polyA). (A) Quantitative immunoblotting of heart homogenates from HAX-1 overexpressors (OE) and wild-type (WT). (B) Immunofluorescence analysis of HAX-1 localization in cardiomyocytes from WT and OE mice, using PLN as a SR marker. To analyze the contractile function, cardiomyocytes from OE or age-matched WT mice were isolated; contractility and calcium transients were recorded and analyzed under basal conditions (Basal) and upon isoproterenol stimulation (Iso, 100 nM). (C, E, and G) Percentage of fractional shortening (FS%), rate of contraction (PdL/dt, $\mu\text{m}/\text{s}$) and rate of relaxation (NdL/dt, $\mu\text{m}/\text{s}$). (D) Calcium amplitude, indicated by fura-2 ratio of 340/380 nm. (F) Tau. (H) Peak of SR calcium load, indicated by the fura-2 ratio of 340/380 nm. (I) Initial rates of oxalate-supported SR Ca uptake in cardiac homogenates from WT (\square) and OE (\bullet) mice. (Inset) The EC_{50} of SERCA for calcium in OE and WT hearts. Values were normalized to V_{max} values. (J) Representative immunoblots (upper panel) and relative protein levels (lower panel) of PLN monomers and pentamers in WT and OE heart homogenates. Data are mean \pm SEM. $n = 6-8$ hearts for each group (for C-H, 8-10 cells/heart). *, $P < 0.05$, compared to wild-type hearts.

well as calcium transients were evaluated (13). Overexpression of HAX-1 resulted in significantly depressed fractional shortening and rates of contraction and relaxation to 52, 42 and 44% of wild-type, respectively (Fig. 2C, E, and G). However, the maximal stimulated contractile parameters from HAX-1 overexpressing and wild-type cells were similar in the presence of isoproterenol (Fig. 2C, E, and G). Contractility studies in cardiomyocytes from line 13 yielded the same results as those of line 11 (Fig. S3 A-C). Therefore, the following studies were performed using line 11.

Consistent with the inhibitory effects of HAX-1 in mechanical performance, the peak of calcium transient was decreased to 67%

and tau was prolonged to 136% of wild-type, respectively (Fig. 2D and F). The depressive effects of HAX-1 were abolished by isoproterenol stimulation (Fig. 2D and F). Thus, in vivo overexpression of HAX-1 inhibited SR calcium cycling and contractile performance under basal conditions without any significant effects upon maximal isoproterenol stimulation.

Examination of the caffeine-induced SR calcium release revealed that overexpression of HAX-1 significantly decreased calcium load to 77% of wild-type, while isoproterenol prevented this inhibition (Fig. 2H).

Effects of HAX-1 Overexpression on SR Ca Transport. Since HAX-1 has been shown to interact with PLN (5), we assessed the effects of HAX-1 on oxalate-supported SR calcium transport. HAX-1 overexpression resulted in significant decreases in the initial rates of calcium transport at various calcium concentrations without any marked alterations in the maximal velocity of the uptake system, compared to wild-type (WT: 75.23 ± 8.84 nmol/mg/min; OE: 81.62 ± 7.69 nmol/mg/min) (Fig. 2I). However, the EC_{50} of SERCA2 for calcium was increased by 39% in the HAX-1 transgenic hearts (Fig. 2I Inset), which was associated with increases in the relative PLN monomer/pentamer ratio (Fig. 2J). Total PLN levels were similar between WT and transgenic hearts (Fig. S4). Thus, the active PLN monomeric species was significantly higher in the transgenic hearts.

The alterations in SR calcium cycling by HAX-1 were not associated with any differences in the major SR calcium cycling protein levels, such as SERCA2, total PLN, phosphorylated PLN at Ser¹⁶ or Thr¹⁷, total ryanodine receptor, as well as phosphorylated ryanodine receptor at Ser²⁸⁰⁹ (Fig. S4).

Role of HAX-1 Gene Targeting on Cardiomyocyte Contractile Function.

To further investigate the effects of HAX-1 on cardiac contractile performance in vivo, a HAX-1-deficient mouse model (14) was characterized. The homozygous mice died between 5 and 12 weeks of age. However, the heterozygous mice with 36% HAX-1 expression levels in the heart (Fig. S5 A and B) were viable and fertile (14) and used to perform the following study.

HAX-1 heterozygous cardiomyocytes showed significantly increased fractional shortening and rates of contraction and relaxation to 138, 145, and 156%, respectively, compared to age matched wild-types under basal conditions (Fig. 3A, C, and E). However, there were no marked differences in these contractile parameters upon isoproterenol stimulation (Fig. 3A, C, and E). Accordingly, the peak of the calcium transient was significantly increased to 158%, and the time to 50% decay of calcium as well as tau were shortened to 77 and 72% of wild-type under basal conditions. There were no significant alterations of these calcium parameters upon isoproterenol stimulation (Fig. 3B, D, and F). Furthermore, the SR calcium load, assessed by caffeine-induced SR calcium release, was increased 13% in the HAX-1 heterozygous, compared to wild-type cells (Fig. 3G). These differences were abolished upon isoproterenol stimulation (Fig. 3G).

We then examined the role of HAX-1 downregulation on SR Ca transport. Decreased HAX-1 expression resulted in significant increases in the initial rates of calcium transport at various calcium concentrations without any marked alterations in the maximal velocity of the uptake system, compared to wild-type (WT: 85.4 ± 6.6 nmol/mg/min; HE: 83.2 ± 5.9 nmol/mg/min) (Fig. 3H). However, the EC_{50} of SERCA2 for calcium was significantly decreased to 64% in the HAX-1 heterozygous mouse hearts, compared to wild-type (Fig. 3H, inset).

The alterations in SR calcium cycling by HAX-1 downregulation were not associated with any differences in the major SR calcium cycling protein levels: SERCA2a, calsequestrin (CSQ), and PLN (Fig. S5A). Furthermore, there were no significant changes in cardiac morphology and histology at the age of 3 months in the HAX-1 heterozygous mice, compared to WTs (Fig. S5C).

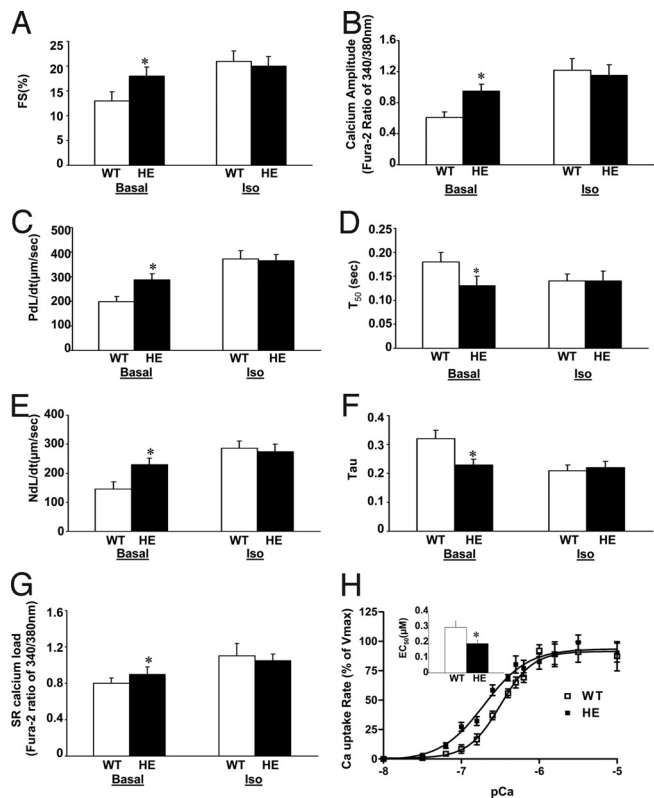


Fig. 3. Effect of HAX-1 deficiency on cardiomyocyte contractile function. Cardiomyocytes from HAX-1 heterozygous mice (HE) or age-matched wild-type (WT) were isolated; contractility and calcium transients, as well as caffeine-induced calcium release from SR were recorded and analyzed. (A, C, and E) Percentage of fractional shortening (FS%), rate of contraction (PdL/dt, $\mu\text{m}/\text{s}$) and rate of relaxation (NdL/dt, $\mu\text{m}/\text{s}$). (B) Calcium amplitude, indicated by the fura-2 ratio of 340/380 nm. (D) Time to 50% decay of calcium (T_{50} , s). (F) Tau. (G) Peak of SR calcium load, indicated by the fura-2 ratio of 340/380 nm. A–G are all under basal conditions (Basal) and upon isoproterenol stimulation (Iso). (H) Initial rates of oxalate-supported SR calcium uptake in hearts from WT (\square) and HE (\blacksquare) mice. (H, inset) The EC₅₀ of SERCA for calcium in HE and WT hearts. Data are mean \pm SEM. $n = 4$ –6 hearts for each group (for A–G, 8–10 cells/heart). *, $P < 0.05$, compared to wild-type hearts.

Effect of HAX-1 on the Interactions of PLN to PLN and PLN to SERCA.

Our previous data have shown that HAX-1 interacts with PLN (5). However, it is not clear whether HAX-1 may affect PLN's interaction with itself (oligomerization, “K_{D1}”), or it may alter the ability of PLN to bind SERCA2 (“K_{D2}”) in SR membranes. To directly test the effect of HAX-1 on these linked binding equilibria, we fused fluorescent protein tags to the N-termini of SERCA and PLN, and measured fluorescence resonance energy transfer (FRET), using the acceptor photobleaching method (15, 16). Fig. 4A shows fluorescence images of CFP-SERCA and YFP-PLN in cultured AAV-293 cells. After acceptor-selective photobleaching, YFP-PLN fluorescence was decreased and CFP-SERCA fluorescence was increased, indicating the CFP donor had been quenched by energy transfer to YFP-PLN. Quantification of time-series image data showed that the exponential photobleaching of YFP-PLN (Fig. 4B, green triangles) resulted in a concomitant increase in CFP-SERCA (Fig. 4B, blue circles). However, upon cotransfection, CFP-SERCA fluorescence was further enhanced with HAX-1 (Fig. 4B, black squares). This suggests that HAX-1 increased FRET from CFP-SERCA to YFP-PLN compared to control. Conversely, intrapentameric FRET from CFP-PLN to YFP-PLN was decreased in the presence of HAX-1 (Fig. 4C). Our FRET results are summarized in Fig. 4D and indicate that HAX-1 decreased average intrapentameric (PLN-PLN) FRET efficiency and increased average reg-

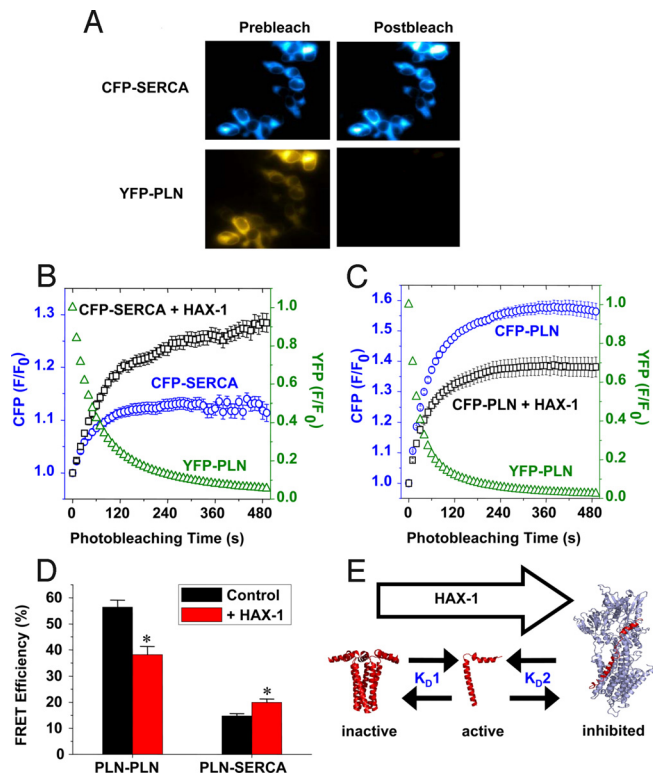


Fig. 4. Effect of HAX-1 on PLN-PLN and PLN-SERCA fluorescence resonance energy transfer (FRET). (A) Fluorescence microscopy showed that acceptor-selective photobleaching of YFP-PLN fluorescence resulted in an increase in CFP-SERCA fluorescence, indicating FRET. (B) Image quantification showed CFP-SERCA fluorescence (blue circles) increased exponentially as YFP-PLN (green triangles) was photobleached. The magnitude of CFP-SERCA fluorescence enhancement was greater in cells cotransfected with HAX-1 (black squares), suggesting increased FRET compared to control. (C) CFP-PLN fluorescence (blue circles) increased as YFP-PLN (green triangles) was bleached, indicating intrapentameric FRET. The magnitude of the CFP-PLN fluorescence enhancement was smaller in cells cotransfected with HAX-1 (black squares), suggesting reduced FRET. (D) Summary of FRET microscopy results. Coexpression of HAX-1 caused a 32% decrease in overall FRET between CFP-PLN and YFP-PLN, and a 35% increase in overall FRET between CFP-SERCA and YFP-PLN. Data are mean \pm SEM, *, $P < 0.01$, compared with control. (E) A model for HAX-1 regulation of cardiac calcium handling. HAX-1 shifts the PLN pentamer/monomer equilibrium toward the active, monomeric species, and promotes formation of the PLN-SERCA regulatory complex.

ulatory complex (PLN-SERCA) FRET efficiency. The observed 30% decrease in PLN-PLN FRET is consistent with the observed decrease in pentamer/monomer ratio in HAX-1 OE transgenic hearts (Fig. 2J). These data support a model in which HAX-1 stabilizes the SERCA-PLN regulatory complex and/or destabilizes the oligomeric PLN complex (Fig. 4E). Shifting these linked binding equilibria (Fig. 4E, “K_{D1}” and “K_{D2}”) to the right is expected to increase functional inhibition of SERCA by PLN (4).

Effects of HAX-1 Overexpression in the Absence of PLN. Our findings above indicate that the interaction between PLN and HAX-1 may play an important role in mediating the depressive effects of HAX-1 on SR calcium cycling. To confirm this hypothesis, we generated a cross model with HAX-1 overexpression in the PLN deficient background (OE/KO). The levels of HAX-1 overexpression were similar to those in the original HAX-1 transgenic hearts. Interestingly, HAX-1 had no effect on cardiomyocyte contractility and calcium transients as well as SR calcium content in the absence of PLN (Fig. 5 A–E). Furthermore, the affinity of SERCA2 for calcium (EC₅₀) was similar between the cross model and the PLN

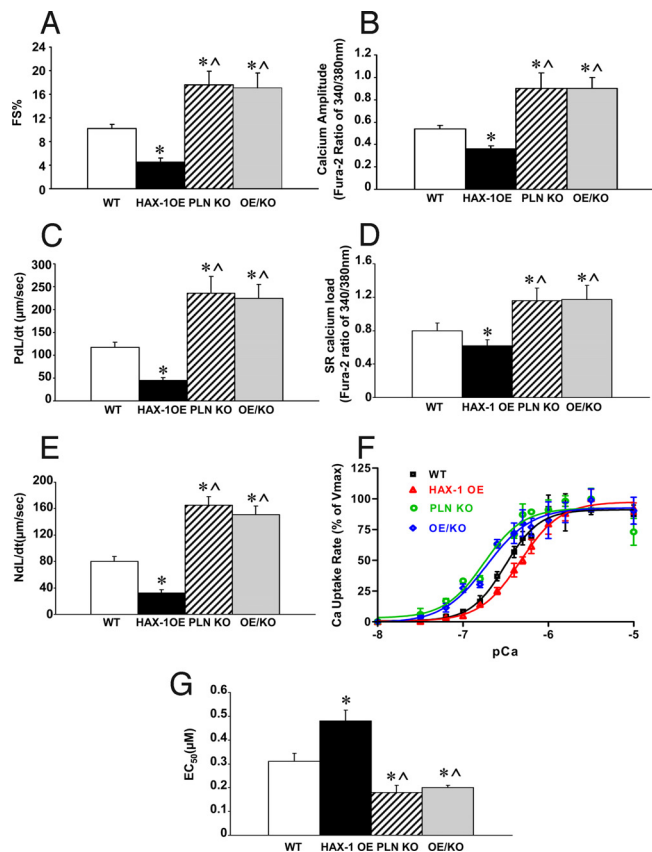


Fig. 5. Effect of HAX-1 overexpression on cardiomyocyte contractile performance in the absence of PLN. Cardiomyocytes were isolated from HAX-1 overexpression in the PLN knockout background (OE/KO), PLN knockout (PLN KO), and HAX-1 overexpression (HAX-1 OE) mice as well as age-matched wild-type (WT). Contractility and calcium transients as well as caffeine-induced SR calcium release from SR were recorded and analyzed. (A) Percentage of fractional shortening (FS%); (C) Rate of contraction (PdL/dt, $\mu\text{m/s}$); and (E) Rate of relaxation (NdL/dt, $\mu\text{m/s}$). (B) Calcium amplitude, indicated by the fura-2 ratio of 340/380 nm. (D) Peak of SR calcium load, indicated by the fura-2 ratio of 340/380 nm. A–E are all under basal conditions. Data are mean \pm SEM, $n = 4$ –5 hearts (8–10 cells/heart) for each group. (F) Initial rates of oxalate-supported SR calcium uptake, and (G) EC_{50} of calcium uptake in heart homogenates from WT, HAX-1 OE, PLN KO and OE/KO mice. Data are mean \pm SEM. $n = 6$ –8 hearts for each group. *, $P < 0.05$, compared to WT. ^, $P < 0.05$, compared to HAX-1 OEs.

KO hearts (Fig. 5 F and G). These data suggest that the role of HAX-1 on cardiac calcium cycling and contractile function is dependent on the presence of PLN. To investigate the localization of HAX-1 in this cross model, we performed immunofluorescence studies in the isolated cardiomyocytes from WT, HAX-1 OE, and OE/KO mice. Our results indicate that HAX-1 colocalizes with both SR marker SERCA and Mito Tracker in these mouse models (Fig. S6).

Discussion

The current study presents evidence that the anti-apoptotic protein HAX-1 decreases cardiac contractile parameters and calcium kinetics through increased PLN inhibition of the SR calcium transport system, mediated by formation of PLN monomers. However, isoproterenol stimulation, associated with PLN phosphorylation, relieves these inhibitory effects of HAX-1. A previous study, using the yeast two-hybrid system, identified HAX-1 as a binding partner of PLN (5). The PLN binding region by HAX-1 contains residues 16–22, which include both the Ser¹⁶ and Thr¹⁷ phosphorylation sites. Notably, this domain does not contain the PLN interaction sites with SERCA2 (17, 18).

However, amino acids 16–22 in PLN contain Ile-18, Glu-19, Met-20, and Pro-21, which form a turn to connect the two α -helical stretches of the protein (19). The formation of this turn in PLN provides flexibility, which may play an important role in the kinetics of PLN monomer-pentamer formation, phosphorylation, and dephosphorylation (19). Thus, binding of HAX-1 to this region may alter any of the above reactions to further affect PLN conformation and activity. Indeed, the present study demonstrates that cardiac overexpression of HAX-1 significantly increased the relative abundance of PLN monomers, indicating an enhanced inhibitory role of PLN for SERCA, which subsequently resulted in depressed SERCA2 affinity for calcium. This was also confirmed by an in vitro FRET study, in which HAX-1 could significantly diminish the interaction between PLN monomers but increase the interaction between PLN and SERCA2. It has been previously reported that mutations of PLN itself including Leu³⁷ to Ala, Ile⁴⁰ to Ala, and Asn²⁷ to Lys, lead to increased PLN monomeric forms and enhance its inhibitory role in SERCA activity and cardiac function (13, 20). The present study suggests that HAX-1 may also function as a signal to control the transition of the spatial conformation of PLN in the SR, which may further regulate SR calcium cycling. The increased inhibitory activity of PLN by HAX-1 overexpression resulted in decreased SR calcium load and depressed cardiomyocyte calcium cycling as well as contractility. Accordingly, downregulation of HAX-1 in vitro and in vivo enhanced calcium kinetics and mechanical parameters, supporting the regulatory role of HAX-1 in cardiac contractile function. Furthermore, these effects appeared to be specifically mediated by PLN, since PLN phosphorylation or ablation prevented the HAX-1 inhibitory activity.

In the current study, we did not find any significant effects of the overexpressed HAX-1 on the phosphorylation status of PLN at Ser-16 and Thr-17, indicating that the depressed function was associated with binding of HAX-1 to PLN. Importantly, the inhibitory effects of HAX-1 overexpression were eliminated by isoproterenol stimulation, which may be a consequence of dissociation of HAX-1 from PLN (5). Indeed, phosphorylation of PLN at both Ser-16 and Thr-17 was similar in transgenic and wild-type hearts in the presence of isoproterenol. In addition, genetic complementation studies indicated that HAX-1 overexpression had no effects in the PLN deficient hearts. Thus, although HAX-1 has been previously shown to interact with both PLN and SERCA (5, 21), the present findings indicate that the PLN/HAX-1 interaction is key in mediating the inhibition of SR calcium cycling by HAX-1 in vivo. The major effects of HAX-1 on SR calcium transport involved the EC_{50} of SERCA for calcium, which is known to be regulated by PLN, rather than the maximal velocity of SERCA, which reflects direct SERCA regulation (22, 23).

PLN has been recognized as an important brake control in SR, which keeps SERCA2a partially inhibited under basal conditions and allows for increased SR calcium transport under β -adrenergic stimulation, when PLN inhibition is relieved. However, it needs to be understood whether or not PLN is the only regulator of SERCA activity. The current study demonstrates that HAX-1 may serve as an additional control of SERCA function. This adds another layer of complexity as HAX-1 interacts with PLN and increases its inhibitory function. It is interesting to speculate that HAX-1 interacts with PLN and keeps it in its monomeric form, which is the inhibitory form of PLN, and thus, represents an important regulator of cardiac reserve. Although it has been reported that protein kinase A-induced phosphorylation of PLN led to dissociation of HAX-1 in vitro (5), it remains unclear whether this also holds true in vivo. It is possible that phosphorylation of PLN alters its spatial conformation and promotes pentameric formation, which then changes the affinity of PLN for HAX-1. Alternatively, PLN phosphorylation may reduce the interaction of monomeric PLN for HAX-1 and lead to pentameric assembly. Along these lines, the

simplest model consistent with our data are that HAX-1 binds independently to monomeric PLN (via HAX-1 residues 203–225) and to SERCA (via HAX-1 residues 203–245) (21). Binding of HAX-1 to PLN monomers induces depolymerization of PLN (Figs. 2J and 4D) (24), while simultaneous binding of HAX-1 to PLN and SERCA in a ternary complex stabilizes the PLN-SERCA interaction (Fig. 4D). This putative ternary complex must preserve the functional inhibitory contact between the SERCA pump and PLN (Fig. 2I).

HAX-1 has been recognized as an anti-apoptotic protein mainly through the mitochondria pathway (8). However, the ER/SR localization of HAX-1 may provide another mechanism for its anti-apoptotic action. Indeed, the anti-apoptotic effects of Bcl-2 are associated with decreasing SR calcium content through increased SR calcium leak (25). Along these lines, we did not find any significant differences in SR calcium leak, assessed by calcium sparks in HAX-1 overexpressing cardiomyocytes, compared to wild-type. Nevertheless, SR calcium load was decreased, similar to Bcl-2, but the effect of HAX-1 was mainly mediated by its interaction with PLN. The lack of HAX-1 inhibition in the PLN deficient background provides further evidence about this notion. The decreased SR calcium content by HAX-1 may be associated with reduced mitochondria calcium load or permeability transition pore potential, similar to Bcl-2 (25), leading to cardioprotection.

In this study, we found that HAX-1 colocalized with PLN in SR and Cox IV in mitochondria. HAX-1 has been previously reported to interact with SERCA and PLN (5, 21). Interestingly, studies in HEK 293 cells have shown that HAX-1 colocalizes with PLN and SERCA at the ER compartment, only with the presence of PLN in ER (5, 21). HAX-1 was also reported to localize in the cytoplasm

(26). However, based on many known interaction partners of HAX-1, the variety of cellular functions and the existence of multiple HAX-1 isoforms, the localization of HAX-1 might vary in different cell types (26, 27).

In summary, the current study demonstrated a functional role of HAX-1 in cardiomyocytes. A number of complementary approaches, including acute adenoviral gene transfer, transgenesis, gene targeting, and gene complementation were used to elucidate the mechanisms underlying regulation by HAX-1. Our findings suggest that HAX-1 modulates cardiomyocyte SR calcium transport and contractility, through a dynamic interaction with PLN (Fig. S7). Thus, the PLN/HAX-1 complex provides an additional layer of regulation in calcium cycling and contractility in the heart.

Materials and Methods

Sense and anti-sense HAX-1 adenoviruses were generated and used to infect isolated adult rat cardiomyocytes. HAX-1 transgenic mice (FVB/N) were generated by standard procedures (13). Heterozygous HAX-1-deficient mice were purchased from St. Jude's Children Research Hospital (14). HAX-1 transgenic mice (FVB/N) were also crossed with PLN deficient mice (FVB/N) to generate a cross mouse model with HAX-1 overexpression in the PLN knockout background (FVB/N). Cardiac contractile and calcium kinetic parameters were determined by isolated adult rat or mouse cardiomyocytes (13). Animals were handled and maintained according to protocols by the ethics committee of the University of Cincinnati. The investigation conforms to the Guide for the Care and Use of Laboratory Animals published by the National Institutes of Health. Detailed description of methods is available in *SI Text*.

ACKNOWLEDGMENTS. The authors thank Dr. Donald M. Bers for fruitful discussions and Dr. Guoxiang Chu's nice suggestion in writing. This work was supported by National Institutes of Health Grants HL-26057, HL-64018, HL-77101, by the Leducq Foundation (to E.G.K.), and by an American Heart Association Post-Doctoral Fellowship (to J.R.W.).

- Dash R, et al. (2001) Interactions between phospholamban and beta-adrenergic drive may lead to cardiomyopathy and early mortality. *Circulation* 103:889–896.
- Haghighi K, et al. (2001) Superinhibition of sarcoplasmic reticulum function by phospholamban induces cardiac contractile failure. *J Biol Chem* 276:24145–24152.
- Zhai J, et al. (2000) Cardiac-specific overexpression of a superinhibitory pentameric phospholamban mutant enhances inhibition of cardiac function in vivo. *J Biol Chem* 275:10538–10544.
- MacLennan DH, Kranias EG (2003) Phospholamban: A crucial regulator of cardiac contractility. *Nat Rev Mol Cell Biol* 4:566–577.
- Vafiadaki E, et al. (2007) Phospholamban interacts with HAX-1, a mitochondrial protein with anti-apoptotic function. *J Mol Biol* 367:65–79.
- Suzuki Y, et al. (1997) HAX-1, a novel intracellular protein, localized on mitochondria, directly associates with HS1, a substrate of Src family tyrosine kinases. *J Immunol* 158:2736–2744.
- Fadeel B, Grzybowska E (2009) HAX-1: A multifunctional protein with emerging roles in human disease. *Biochim Biophys Acta* 1790:1139–1148.
- Han Y, et al. (2006) Overexpression of HAX-1 protects cardiac myocytes from apoptosis through caspase-9 inhibition. *Circ Res* 99:415–423.
- Dufva M, Olsson M, Rymo L (2001) Epstein-Barr virus nuclear antigen 5 interacts with HAX-1, a possible component of the B-cell receptor signaling pathway. *J Gen Virol* 82:1581–1587.
- Gallagher AR, Cedzich A, Gretz N, Somlo S, Witzgall R (2000) The polycystic kidney disease protein PKD2 interacts with Hax-1, a protein associated with the actin cytoskeleton. *Proc Natl Acad Sci USA* 97:4017–4022.
- Klein C, et al. (2007) HAX1 deficiency causes autosomal recessive severe congenital neutropenia (Kostmann disease). *Nat Genet* 39:86–92.
- Sharp TV, et al. (2002) K15 protein of Kaposi's sarcoma-associated herpesvirus is latently expressed and binds to HAX-1, a protein with antiapoptotic function. *J Virol* 76:802–816.
- Zhao W, et al. (2006) The presence of Lys27 instead of Asn27 in human phospholamban promotes sarcoplasmic reticulum Ca²⁺-ATPase superinhibition and cardiac remodeling. *Circulation* 113:995–1004.
- Chao JR, et al. (2008) Hax1-mediated processing of HtrA2 by Parl allows survival of lymphocytes and neurons. *Nature* 452:98–102.
- Hou Z, Kelly EM, Robia SL (2008) Phosphomimetic mutations increase phospholamban oligomerization and alter the structure of its regulatory complex. *J Biol Chem* 283:28996–29003.
- Kelly EM, Hou Z, Bossuyt J, Bers DM, Robia SL (2008) Phospholamban oligomerization, quaternary structure, and sarco(endo)plasmic reticulum calcium ATPase binding measured by fluorescence resonance energy transfer in living cells. *J Biol Chem* 283:12202–12211.
- Kimura Y, Asahi M, Kurzydowski K, Tada M, MacLennan DH (1998) Phospholamban domain Ib mutations influence functional interactions with the Ca²⁺-ATPase isoform of cardiac sarcoplasmic reticulum. *J Biol Chem* 273:14238–14241.
- Toyofuku T, Kurzydowski K, Tada M, MacLennan DH (1994) Amino acids Glu2 to Ile18 in the cytoplasmic domain of phospholamban are essential for functional association with the Ca²⁺-ATPase of sarcoplasmic reticulum. *J Biol Chem* 269:3088–3094.
- Pollesello P, Annala A, Ovaska M (1999) Structure of the 1–36 amino-terminal fragment of human phospholamban by nuclear magnetic resonance and modeling of the phospholamban pentamer. *Biophys J* 76:1784–1795.
- Zvaritch E, et al. (2000) The transgenic expression of highly inhibitory monomeric forms of phospholamban in mouse heart impairs cardiac contractility. *J Biol Chem* 275:14985–14991.
- Vafiadaki E, et al. (2009) The Anti-apoptotic protein HAX-1 interacts with SERCA2 and regulates its protein levels to promote cell survival. *Mol Biol Cell* 20:306–318.
- Fan GC, Gregory KN, Zhao W, Park WJ, Kranias EG (2004) Regulation of myocardial function by histidine-rich, calcium-binding protein. *Am J Physiol Heart Circ Physiol* 287:H1705–1711.
- Gregory KN, et al. (2006) Histidine-rich Ca binding protein: A regulator of sarcoplasmic reticulum calcium sequestration and cardiac function. *J Mol Cell Cardiol* 40:653–665.
- Reddy LG, Jones LR, Thomas DD (1999) Depolymerization of phospholamban in the presence of calcium pump: A fluorescence energy transfer study. *Biochemistry* 38:3954–3962.
- Pinton P, et al. (2000) Reduced loading of intracellular Ca²⁺ stores and downregulation of capacitative Ca²⁺ influx in Bcl-2-overexpressing cells. *J Cell Biol* 148:857–862.
- Hippe A, et al. (2006) Expression and tissue distribution of mouse Hax1. *Gene* 379:116–126.
- Ortiz DF, et al. (2004) Identification of HAX-1 as a protein that binds bile salt export protein and regulates its abundance in the apical membrane of Madin-Darby canine kidney cells. *J Biol Chem* 279:32761–32770.